第 24 卷第 3 期 无 机 化 学 学 报 Vol.24 No.3
2008 年 3 月 CHINESE JOURNAL OF INORGANIC CHEMISTRY 340~350

氧分子在 $Cu_2O(111)$表面吸附与解离的理论研究

孙宝珍[1] 陈文凯*,[1] 王 霞[1] 李 奕[1] 陆春海[2]
([1]福州大学化学系,福州 350108)
([2]中国工程物理研究院,绵阳 621900)

摘要: 本文采用密度泛函方法结合周期性平板模型,研究了氧原子和氧分子在完整和存在缺陷的 $Cu_2O(111)$表面的吸附。计算结果表明氧原子倾向于吸附在配位饱和的 Cu_{CSA} 位,而对于氧分子,则强烈倾向于吸附在配位不饱和的 Cu_{CUS} 位。氧分子在含有氧空位的缺陷表面的优势吸附位为平行吸附于空位上方的桥位。过渡态的计算表明氧分子在缺陷表面的解离是一个活化能很小的放热过程。

关键词: 氧; 氧化亚铜表面; 密度泛函理论; 平板模型; 解离; 吸附
中图分类号: O614.121 **文献标识码**: A **文章编号**: 1001-4861(2008)03-0340-11

A Theoretical Study of O_2 Adsorption and Dissociation on $Cu_2O(111)$ Surface

SUN Bao-Zhen[1] CHEN Wen-Kai*,[1] WANG Xia[1] LI Yi[1] LU Chun-Hai[2]
([1]Department of Chemistry, Fuzhou University, Fuzhou 350108)
([2]China Academy of Engineering Physics, Mianyang, Sichuan 621900)

Abstract: Interaction of atomic and molecular oxygen with perfect and defective Cu_2O (111) surfaces has been studied by periodic density functional theory coupled with slab models. Different kinds of possible modes of O and O_2 adsorbed on Cu_2O (111) surface and possible dissociation pathways were calculated. Meanwhile, different electronic states, i.e., the singlet and the triplet states were considered in the computation. The optimization of the geometry, calculation of the adsorption energy, vibrational frequency and analysis of the Mulliken population were carried out. The results indicate that Cu_{CSA} site is slightly more favorable than Cu_{CUS} for O adsorption, and for O_2 adsorption over perfect surface, Cu_{CUS} site is the most advantageous position, especially for O_2 with end-on type. For O_2 adsorption over the deficient surface, it has a larger adsorption energy compared to O_2 adsorption over the perfect surface and the O-O bond strength is considerably weakened when O_2 lies flatly on the oxygen vacancy site and lies flatly over 1-vacancy bridge site. And the oxygen adspecies is characteristic of a classical O_2^- ion on perfect surface, whereas is O_2^{2-} ion on oxygen-deficient surface. The calculations for transition states show that the dissociation reaction of O_2 on deficient surface is highly exothermic with a very small barrier height.

Key words: oxygen; $Cu_2O(111)$; density functional theory; slab models; dissociation; adsorption

收稿日期: 2007-08-13。**收修改稿日期**: 2007-12-20。
国家自然科学基金委员会-中国工程物理研究院联合基金(No.10676007),**福建省高等学校新世纪优秀人才支持计划和福建省自然科学基金**(No.U0650012)**资助**。
* **通讯联系人**。E-mail: qc2008@fzu.edu.cn; Tel: +86-591-87892522
第一作者: **孙宝珍**, **女**, 27 **岁**, **硕士研究生**; **研究方向**: **应用量子化学**。

0 Introduction

The adsorption of gas-phase oxygen at oxide surfaces plays an important part in many types of heterogeneous catalysis[1,2]. Because of its promising applications in solar energy conversion and catalysis[3~8], copper (I) oxide (Cu_2O) has been studied by many researchers. There has been much interest in Cu_2O due to its electronic structure [9,10]. Details about the interact-ion and reaction of small molecules with Cu_2O surface is important for chemists to understand the electronic structure of Cu_2O, as well as the mechanism of the catalytic processes. Some small molecules, such as CO, NO and H_2O, adsorbed on Cu_2O were studied by both experimental and theoretical methods[11~21]. However, many of these studies were focused on Cu_2O perfect surfaces, little of them have been done for defective surfaces [22]. In fact, the important properties of most metal oxides, including surface reactivity, are closely connected to the presence of defects. For example, the presence of oxygen vacancies on the NiO (100) surface leads to an increase in the adsorption energy of H_2 and lowers the energy barrier for cleavage of H-H bond[23]. In contrast, a perfect NiO (100) surface exhibits the negligible reactivity towards H_2. Moreover, it also should be noted that a few studies of O_2 adsorption on Cu_2O surface have been reported[9], but several reports of O_2 adsorption on other metal oxides and metal surfaces have been done[24~36]. Schulz et al. experimentally investigated O_2 adsorption on Cu_2O(111) perfect and defective surfaces by photoemission and low energy electron diffraction (LEED)[9]. For a detailed understanding of the surface process, experimental information is however not always sufficient and accompanying theoretical calculations can be helpful to clarify some of the open questions.

The major issue that we address is determination of the preferred adsorption site of atomic and molecular oxygen on perfect and deficient surfaces and the dissociation process of O_2 on the defective surface. Experiments have clearly shown that the adsorption of O_2 at room temperature was found to be molecular adsorption on stoichiometric (111) surfaces, and to be dissociative adsorption on defected (111) surfaces prepared by ion bombardment, whereas the adsorption geometry and behaviour of atomic oxygen and molecular oxygen or the role of the surface defect is less well understood. To complement the experimental results we use density functional method to get deeper microscopic insight into the interaction of O_2 with Cu_2O (111) perfect and defective surfaces. Herein, we report calculations for both the singlet and triplet states. To the best of our knowledge, such calculations have not been reported so far.

1 Computational models and methods

1.1 Surface models

Fig.1a and Fig.1b show the stoichiometric Cu_2O (111) surface. The ideal, stoichiometric, Cu_2O (111) surface is nonpolar including four chemically distinguishable types of surface atoms which were denoted as Cu_{CUS}, Cu_{CSA}, O_{SUF} and O_{SUB} shown in Fig.1a. The Cu_{CUS} is the surface copper that is coordinatively unsaturated, i.e. singly-coordinate Cu^+ cations (bulk Cu^+ coordination number=2), which acts as a Lewis acid site. Cu_{CSA} is the coordinatively saturated copper atom, i.e. doubly-coordinate Cu^+. O_{SUF} is the outer-most surface oxygen, i.e. threefold-coordinate oxygen anions (bulk lattice O^{2-} coordination number=4), which acts as a Lewis base site. And O_{SUB} is the subsurface oxygen, i. e. fourfold-coordinate oxygen anions. The Cu_{CUS} and the O_{SUF} constitute Lewis acid-base pairs, they are the adsorption active centers[18].

Experimental results[9] suggest Cu_2O(111) surface have two different surface terminations, one is in (1×1) periodicity (see Fig.1a) and another is in $(\sqrt{3}\times\sqrt{3})$R30° periodicity (see Fig.1b). And the (1×1) surface prepared by ion bombardment and annealing gives about 3% oxygen vacancies in the top atomic layer, which is similar to the ideal stoichiometric surface. However, $(\sqrt{3}\times\sqrt{3})$R30° periodicity is characteristic of one-third of an atomic layer of oxygen vacancies. Thus, the oxygen-deficient Cu_2O (111) surface can be obtained by removing one oxygen atom in the top atomic oxygen layer from the $(\sqrt{3}\times\sqrt{3})$R30° surface. Each oxygen vacancy gives rise to a

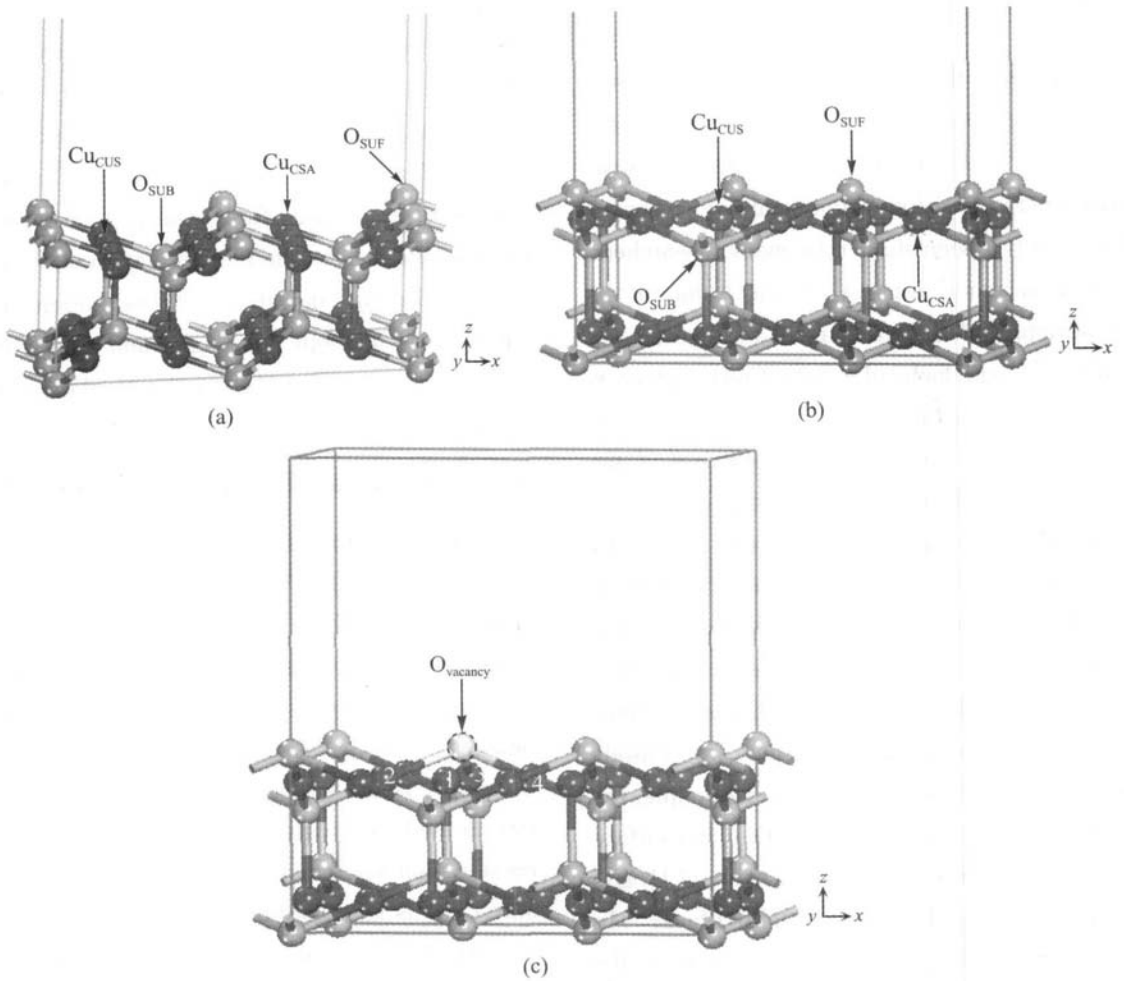

Black circles stand for Cu atoms, the light circles stand for O atoms and the white circles stand for oxygen vacancy

Fig.1 (a) Stoichiometric, $Cu_2O(111)$-(2×2) surface; (b) Stoichiometric, $Cu_2O(111)$-($\sqrt{3}\times\sqrt{3}$)R30° surface; (c) Oxygen-deficient $Cu_2O(111)$-($\sqrt{3}\times\sqrt{3}$)R30° surface

threefold site of singly-coordinate Cu^+ cations. The oxygen-deficient $Cu_2O(111)$-($\sqrt{3}\times\sqrt{3}$)R30° surface is shown as Fig.1c.

Our calculations on the perfect (2×2) and oxygen-deficient ($\sqrt{3}\times\sqrt{3}$)R30° surfaces have been done by using slab models of six layers. The vacuum gap was set to 1 nm, at such a distance there was little interaction between the neighboring layers. In the computation, the substrate was kept fixed to the bulk coordinates. In the next section, we will explain the reason of keeping substrate frozen.

1.2 Computation methods

All calculations were performed using spin-polarized, gradient-corrected, periodic density functional theory (DFT) as implemented in the Dmol[3] software package[37,38]. Exchange and correlation were described within the generalized gradient approximation (GGA) of Perdew and Wang (PW91)[39,40]. It is generally agreed that DFT methods can give quite accurate results for geometry optimization and transition states calculations[41]. This approach has been used in our earlier work on Cu_2O, Au and Cu surfaces[42~47].

In the computation, the inner electrons of copper atoms were kept frozen and replaced by an effective core potential (ECP), the nitrogen and oxygen atoms were treated with an all-electron basis set. The valence electrons functions were expanded into a set of numerical atomic orbitals by a double-numerical basis with polarization functions (DNP). Brillouin-zone integrations have been performed using 3 × 3 × 1 Monkhorst-Pack grid and a Methfessel-Paxton smearing

of 0.005 Ha. The converge criterion judged by the energy, force and displacement, respectively, were 1×10^{-5} Ha, 2×10^{-2} Ha·nm^{-1}, 5×10^{-4} nm. The calculated bond energy and bond length for gas-phase O_2 are 613.22 kJ·mol^{-1} and 0.122 nm, respectively. The corresponding experimental values are 506.63 kJ·mol^{-1} and 0.121 nm[48]. The differences stem mainly from the error in the energy of the free atoms. However, since the density gradients are much lower for the adsorption systems, the description of the energy differences between the reactant state, transition states, and product state is much more accurate than the absolute energy values.

To determine accurate activation barriers, we chose Complete LST/QST approach to search for the transition states of decomposition reactions. The binding energies E_b are defined as:

$$E_b=E_{substrate\text{-}adsorbate}-(E_{substrate}+E_{adsorbate})$$

Where $E_{substrate\text{-}adsorbate}$ is the total energy of adsorbate-substrate system in the equilibrium state, $E_{substrate}$ and $E_{adsorbate}$ is the total energy of substrate and adsorbate (i.e., isolated atomic or molecular oxygen) alone, respectively. By this definition, stable adsorbates will have negative chemisorption energies. The free atomic or molecular oxygen entering this definition is in the true (triplet) ground state, irrespective of whether the adsorbed system is in the singlet or triplet state.

2　Results and discussion

2.1　Surface relaxation

Before calculating the adsorption systems, we firstly considered Cu_2O (111) surface relaxation with $(\sqrt{3}\times\sqrt{3})R30°$ supercell. In this supercell, the lattice parameters are a=b=1.045 8 nm, c=1.369 8 nm. Vectors a, b and c amount to x, y and z axes directions, respectively, as shown in Fig.1. For perfect surface, we examined the structural changes of various adsorption sites. However, for deficient surface, only considered structural changes in the region near a missing oxygen. In this paper, we regard the atoms around the defect site labeled as 1, 2, 3, and 4, respectively. (see Fig.1c). Surface relaxations were found to be minimal and the changes are summarized in Table 1.

Table 1　Changes of atomic coordinate for perfect and deficient surfaces

	Δx / nm	Δy / nm	Δz / nm
CuCUS (1)	0.000 0(0.000 0)	0.000 0(0.051 2)	- 0.012 3(- 0.016 4)
CuCSA (2)	- 0.004 2(0.032 4)	0.002 1(0.032 4)	0.019 2(- 0.013 7)
OSUF (3)	0.000 0(0.000 0)	0.000 0(- 0.032 4))	0.026 0(- 0.013 7)
OSUB (4)	0.000 0(- 0.032 4)	0.000 0(0.000 0)	- 0.024 7(- 0.013 7)

Note: Values listed in the parentheses imply the changes of deficient surface.

For the perfect surface, Cu_{CUS} and O_{SUB} experience an inward displacement of 0.012 3 nm and 0.024 7 nm in the z direction, whereas Cu_{CSA} and O_{SUF} exhibit an opposite movement of 0.019 2 nm and 0.026 0 nm, respectively. Moreover, we can also observe that there is small lateral movement (0.002 1~0.004 2 nm). In other word, the changes are minimal (smaller than 0.005 nm). For the deficient surface, adjacent Cu atoms (2,3 and 4 atoms) near a missing oxygen move inward and sideways (0.013 7 and 0.032 4 nm) to strengthen their bonds with the remain oxygens, 1 atom experiences a relatively larger movement in y and z directions, but still very small. Nevertheless, it has been shown on Cu_2O (111) surface that the lattice relaxation around a vacancy is not very important. Thus, the negligible relaxation is in accordance to the non-polar character of the surface. The geometry of the substrate was kept frozen throughout the calculations.

2.2　Adsorption of atomic O on the Cu_2O(111) surface

The properties of adsorbed atomic oxygen for both the singlet and triplet states are calculated in this study. Five distinct adsorption sites as indicated in Fig.1a and Fig.1c, are explored. In the case of O adsorption at Cu_{CUS}, Cu_{CSA}, O_{SUB} and O_{SUF} sites, the perfect $Cu_2O(111)$-2×2 surface was chosen to employ to calculations, while in the case of $O_{vacancy}$ site, oxygen-deficient $Cu_2O(111)$-$(\sqrt{3}\times\sqrt{3})R30°$ surface was applied to calculations.

The calculated binding energies E_b and the equilibrium distances between O_{ad} and surface adsorption sites are given in Table 2.

Binding energy is always regards as a measure of the strength of adsorbate-surface bonding. From the calculated binding energies listed in Table 2, we could assign the strengths of atomic O adsorption over the five types of pair sites in the following order, O_{ad}-$O_{vacancy}$ > O_{ad}-Cu_{CSA} > O_{ad}-Cu_{CUS} > O_{ad}-O_{SUB} > O_{ad}-O_{SUF}. And O_{ad} coordinated to O_{SUB} and Cu sites is more stable in the triplet than in the singlet state, whereas O_{ad} adsorbed at vacancy and O_{SUF} sites, the binding energy is higher in the singlet state than that in the triplet state. For case of $O_{vacancy}$ site, O_{ad} filled with the vacancy site. It is interesting to compare the relative stability between O_{ad}-Cu_{CUS} and O_{ad}-Cu_{CSA}. Generally speaking, Cu_{CUS} should be more active than Cu_{CSA}. Indeed, the optimized O_{ad}-Cu_{CSA} bond length (see Table 2) is longer than the O_{ad}-Cu_{CUS} distance, whereas the binding energy on the Cu_{CSA} site is higher than that on the Cu_{CUS} site, which reflects the important contribution from the nearby cations. It can be justified by the configuration, which is depicted in Fig.2. In the case of O adsorbed at Cu_{CSA} site, initially the atomic oxygen lies above the Cu_{CSA} site, the configuration was then optimized but the O_{ad} bounds to three Cu atoms, i.e., one Cu_{CUS} and two Cu_{CSA} sites (see Fig.2).

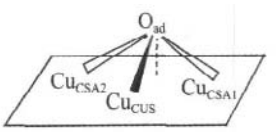

Fig.2 Optimized configuration of atomic O coordinated at Cu_{CSA}

Table 2 Calculated binding energies (kJ·mol^{-1}) and equilibrium distances (unit in pm) for atomic oxygen adsorption on the perfect Cu_2O(111)-(2×2) surface

Multiple state	Site	d(O_{ad}-Cu_{CUS})	d(O_{ad}-Cu_{CSA})	d(O_{ad}-O_{SUF})	d(O_{ad}-O_{SUB})	- E_b
Triplet state	CuCUS	173.2				314.45
	CuCSA	183.3	211.7(211.8)			359.74
	OSUF			146.7		60.81
	OSUB				218.0	153.44
	Ovacancy					610.66
Singlet state	CuCUS	171.6				304.46
	CuCSA	182.4	211.9(212.8)			355.05
	OSUF			147.6		84.70
	OSUB				213.5	132.17
	Ovacancy					654.27

Based on the calculated binding energies, we suspected that there exist in two possible products for the decomposition of O_2 to two O_{ad} atoms on defective Cu_2O (111), one is called product1, i.e., one atomic oxygen is almost completely inserted into the crystal lattice and the other bounds to three Cu atoms. Another is product2, i.e., one O fills with vacancy site and the other adsorbs on Cu_{CUS}.

2.3 Adsorption of O_2 on the perfect Cu_2O(111)-2×2 surface

The adsorption of O_2 in the triplet state was investigated on the perfect Cu_2O (111)-2×2 surface. As we shall show, the interaction of the molecule with surface is always very weak so that the assumption of a triplet ground state should be justified, since this is the ground stated of the free molecule. However, for completeness we also report a few results for adsorption in the singlet state. Two adsorption types of O_2 on the four distinct sites (see Fig.1a) have been considered: an end-on type, involving O_2 perpendicular to the surface, and a side-on type involving O_2 parallel to the surface. The geometries used in the calculations are depicted in Fig.3 and the calculated results are listed in Table 3.

According to Table 3, for the end-on type, a curious feature of a bent structure is observed in M1 and M2, whereas a vertical configuration is seen in M3 and M4. From Table 3, we can also see that in the case of the triplet state, for M1 and M5 they are

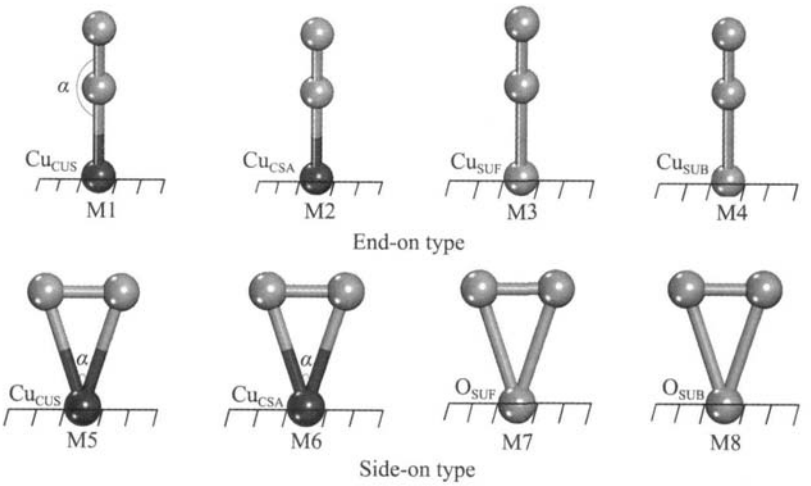

Black circles represent of Cu atoms and the light ones are O atoms

Fig.3　Adsorption geometries for O_2 on the perfect $Cu_2O(111)$-(2×2) surface

Table 3　Properties of O_2 adsorbed at different adsorption sites on $Cu_2O(111)$-(2×2) perfect surface

	Configuration	h / pm	r(O-O) / pm	α / (°)	E_b / (kJ·mol^{-1})	q(O_2)	ν(O-O) / cm^{-1}
Triplet state	M1	188.2	130.5	109	-83.54	-0.227	1 126
	M2	263.3	124.2	120	-1.75		
	M3	342.2	123.3	180	2.82		
	M4	312.7	124.0	180	-1.75		
	M5	193.6	132.5	38	-47.18	-0.246	1 081
	M6	373.3	124.2	21	-2.43		
	M7	333.1	123.1	21	1.88		
	M8	363.0	123.9	19	-1.84		
Singlet state	M1	185.4	136.6	98	-81.70	-0.367	945
	M5	185.3	136.6	98	-81.70	-0.367	945
	Free O_2		122.4				1 555
	O_2^{2-} [49]		149.0				~766
	O_2^- [49]		128.0				~1 097

chemisorption (E_b > 40 kJ·mol^{-1}) and M1 is more favorable than M5 due to its larger adsorption energy and its shorter adsorption height (h). While for other adsorption modes (from M2 to M4 and from M6 to M8), the molecular adsorption energy is very small (no more than 3 kJ·mol^{-1}) and varies rather little with adsorption site and orientation, the adsorbed height, has a large value of typically 260.0 pm, the O-O bond length of adsorbed O_2 molecule changes little with respect to free O_2 molecule (the calculated O-O bond length for free O_2 is 122.0 pm). In the case of singlet state, only the adsorption on the Cu_{CUS} site with end-on and side-on types (i.e., M1 and M5 modes) was taken into account due to the fact that the adsorption on the other sites is a very weak interaction in the triplet state. It is interesting to find that M5 for the singlet state is converted to end-on type after optimization, and M5 mode is same as M1. Moreover, there are only small differences in binding energies and adsorption geometry of M1 between singlet and triplet electronic states. The adsorption energy in the triplet state is slightly larger than that in the singlet state, whereas the O-O distance in the triplet state is slightly shorter than that in the singlet state.

In addition, for M1 and M5, upon adsorption O_2 adspecies are negatively charged, and the intramolecular O-O bond lengths are longer than that of free O_2. In general, the more negative the charges on the O_2

adspecies are, the longer the O-O bond length is, and the more strongly the intramolecular O-O bond is activated by adsorption. And a red-shift of the stretching frequency of the adsorbed O_2 is observed. The trend in vibrational frequency is consistent with that of bond length and Mulliken charges of adsorbed O_2.

Vibrational spectroscopy has suggested the existence of a peroxo form (O_2^{2-}), with a stretching frequency of ~766 cm^{-1}, and a superoxo (O_2^-) form, with a stretching frequency of ~1 097 cm^{-1}. As shown in Table 3, the $\nu(O_2)$ scatters over a wide range from 1130 to 940 cm^{-1}, the O-O distance of adsorbed O_2 (130.0~136.0 pm) is close to that of the O_2^- ion (128.0 pm). All of these indicate that upon adsorption, the oxygen species is assigned to the characteristic of the superoxo (O_2^-) type.

Despite both atomic and molecular oxygen have unpaired electrons and their unoccupied orbitals which can be used to form bonds with the surface, we interestingly find that adsorption of atomic oxygen is more favorable than that of molecular oxygen. This phenomenon is also observed for O_2 adsorption on other metal oxides, such as MgO. Kantorovich et al. have explained the detail reasons [28]. Besides the reasons provided by Kantorovich et al., another likely reason is that it firstly needs to weaken the O-O bond if O_2 forms bonds with the surface, whereas it can directly form bond with surface which needs not to activate the O-O bond firstly for O adsorption. Thus, forming bonds with surface for O is easier than that for O_2.

2.4 Adsorption of O_2 on the oxygen-deficient $Cu_2O(111)$-($\sqrt{3}\times\sqrt{3}$)R30°surface

Since experimental solid surfaces are not always perfect and catalytic processes often occur at surface defects, such as vacancies, steps, and growth islands, we also investigated O_2 adsorption on the defective (111) surface in both the singlet and triplet states. As we mentioned above, the defective surface is obtained by removing one oxygen atom in the top atomic oxygen layer from Cu_2O (111)-($\sqrt{3}\times\sqrt{3}$)R30°surface, the surface defect density is 1/3. This surface exhibits two different kinds of catalytic active adsorption sites subjected to the adsorption of O_2 : Cu_{CUS} and oxygen vacancy sites. Due to the fact that the Cu atoms nearby the oxygen vacancy (i.e., 1, 2, 3, 4 atoms remarked in Fig.1c) are all singly coordination, these Cu atoms belong to the same kind, we believe that the parallel adsorption mode of O_2 at Cu_{CUS} on the deficient surface is unstable. Our calculated results also suggest that after optimization, the initial geometry of O_2 parallel to Cu_{CUS} is converted to O_2 parallel to 1-vacanvy bridge site. Therefore, only five adsorption modes of O_2 on the deficient surface have been considered: a, O_2 lies flatly over the 1~3 bridge site; b, O_2 lies flatly over the 1-vacanvy bridge site; c, O_2 is parallel to vacancy site; d, O_2 is perpendicular to vacancy site; e, O_2 is perpendicular to 1. The adsorption models are depicted in Fig.4 and the corresponding calculated results are given in Table 4.

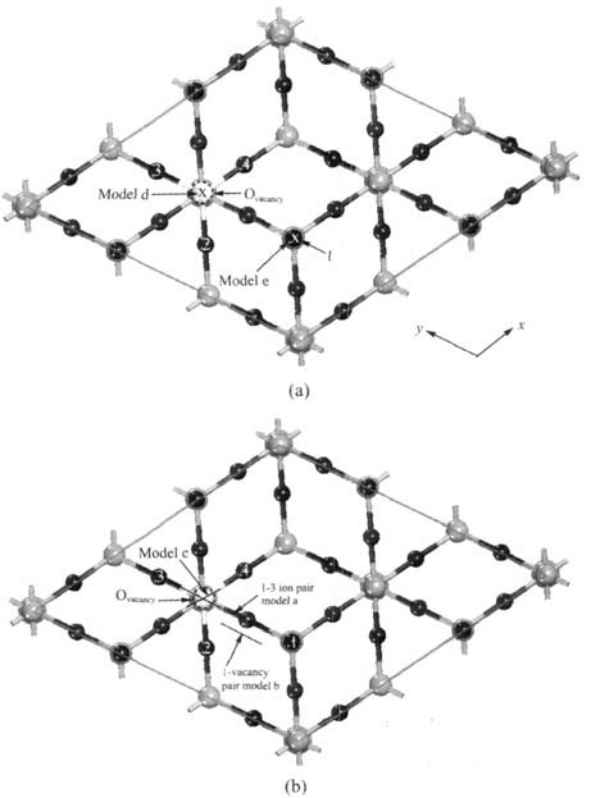

(a) denotes the O_2 upright orientation (×); (b) denotes the O_2 lying-down orientation (—)

Black, light and white circles stand for Cu, O and oxygen vacancy, respectively

Fig.4 Adsorption geometries for the O_2 on the defective (111) surface

On the defective surface, the presence of an

Table 4　Geometrical parameters, binding energies and partial properties for O_2 adsorbed on the deficient surface

	Mode	r(O-O) / pm	E_b / (kJ·mol^{-1})	q(O_2)	ν(O-O) / cm^{-1}
Triplet state	a	272.0	- 362.97	- 0.834	
	b	154.5	- 156.32	- 0.572	497
	c	150.5	- 144.95	- 0.565	668
	d	123.5	- 2.57	- 0.083	1 430
	e	133.8	- 84.51		
Singlet state	a	305.4	- 406.31	- 0.955	
	b	156.0	- 181.48	- 0.596	492
	c	152.6	- 181.61	- 0.600	657
	d	145.6	- 138.13	- 0.616	776
	e	136.9	- 83.87		
Free O_2		122.4			1 555
O_2^{2-}		149.0			~766
O_2^{2-}		128.0			~1 097

oxygen defect induces important changes in the adsorption modes of O_2. Structure e is very similar to structure M1.The binding energies and the O-O bond length in structures a, b and c are all obviously larger than those on the ideal surface. And the O-O bond length in structure d in the triplet state is hardly changed with respect to that calculated for the free molecule and the adsorption energy is much smaller than 40 kJ·mol^{-1}, which is indicative of a weak physisorption, whereas the O-O bond in d in the singlet state is stretched significantly compared to that in the free gas phase and that on the ideal surface, and the adsorption energy is far lager than 40 kJ·mol^{-1},which is a indicative of a strong chemisorption. Namely, for defective surface, both large elongation of the O-O bond and large adsorption energies are obtained. This is particularly important in the case of O_2, because in a kinetic process it will increase the residence time of the molecule on the surface and enhance the probability and rate for O_2 dissociation. Therefore, the $Cu_2O(111)$ surface with oxygen vacancy exhibits a strong chemical reactivity toward to the dissociation of oxygen molecule. As a general speaking, the longer the O-O bond length is, and the more strongly the O-O bond is weaken by adsorption. Such a configuration can contribute to dissociation of O_2. As shown in Table 4, clearly, beside e, the adsorption energies for a mode is the largest, the structure b has almost the same adsorption energy as the structure c and the adsorption energies for d is minimal. In addition, the O-O bond in a is the longest, which is close to the sum of Van der Waals radius of two oxygen atoms, that in b and c is similar, and that in d is the shortest. Thus, in the view of the O-O bond length and the adsorption energies, a, b ,c for both the triplet and singlet states and d only for singlet state are all the favorable modes for O_2 dissociation and a is the most favorable mode for O_2 dissociation. In fact, for a, the rather large bond length of O-O (272.0 pm) indicates that O-O bond has been completely broken. It leads to the mode that an oxygen atom occupy the oxygen defect site and the other oxygen atom adsorbed over Cu_{CUS} site. Moreover, the adsorption energies for a is virtually close to that in the case of atomic oxygen adsorption at Cu_{CUS} site on the ideal surface. Namely, for a, the dissociation of O_2 is spontaneous. However, for b, c and d, despite of the large elongation of the O-O bond, the bond has not been completely broken, the dissociation processes of O_2 virtually need to surmount an energy barrier. If the activation energies required by these decomposition processes are lower than the exothermicities by O_2 adsorption on the deficient surface, the decomposition process would readily occur. In fact, the large exothermicities predicted for these adsorption modes imply a high probability for the occurrence of O_2 decomposition on Cu_2O (111) deficient surface. Usually O_2 does not dissociate on metal oxide

surfaces unless vacancies are present. In this case O_2 dissociation is expected to imply an exothermic process and a small barrier[50].

The corresponding Mulliken charges and the stretching vibrational frequencies of adsorbed O_2 in structures a, b, c, and d are also listed in Table 4. Similar to the case of O_2 adsorption on the ideal surface, for deficient surface, upon adsorption the oxygen molecule carries negative charges and the vibrational frequency of the O-O bond decreases correspond to the free O_2. These changes in Mulliken charges and in the stretching frequency of the O-O bond are consistent with the changes in bond lengths mentioned above. The O-O distance is close to that of the O_2^{2-} ion, 149.0 pm and the ν (O-O) ranges from 490 to 776 cm^{-1}, thereby suggesting that the oxygen adspecies is O_2^{2-} ion. Only for case d in the triplet state, the oxygen adspecies is almost equal to the free O_2 due to its few negative charges.

Comparing adsorption between the triplet state and the singlet state, we point out that for O_2 adsorption on the deficient surface, the triplet electronic state is less stable than the singlet state. Only for case e is the triplet state slightly more stable than the singlet state.

2.5 Decomposition of O_2 on the Cu_2O(111)-($\sqrt{3}\times\sqrt{3}$)R30°oxygen-deficient surface

To gain further detailed understanding of the dissiciative chemisorption process of O_2 on deficient Cu_2O (111) surface, we have calculated the transition states for the dissociation of O_2 to product1 and product2. Herein, the two configurations, b and c, are chosen as the examples to be considered. The transition states were searched by means of complete LST/QST. This method was also employed to study the dissociation of NO dimer at Cu_{CUS} site of the perfect Cu_2O (111) surface[38] and other adsorption reactions occurred on metal surfaces[39]. The calculated reaction and activation energies for O_2 dissociation on the defective (111) surface are shown in Table 5, and the optimized product states, formed from the dissociative adsorption of O_2 over deficient Cu_2O (111) surface, are shown in Fig.5. From Table 5, it can been clearly seen that the dissociation process of O_2 into O subspecies in the two modes of b and c has very small energy barrier. Meanwhile, the dissociative adsorption reaction is highly exothermic. As such, our calculations suggest that the dissociative adsorption of O_2 on the defective (111) surface is much favorable both thermodynamically and kinetically. It is a good agreement with the

Table 5 Reaction and activation energies for O_2 dissociation reactions on defective Cu_2O(111) surface, the O-O distance and Mulliken population of O_2 in the TS structures

	E_a / (kJ·mol^{-1})	$-\Delta E$ / (kJ·mol^{-1})	r(O-O) / pm	q(O_2)
b(T) $\xrightarrow{TS1}$ product 1(T)	0.08	225.88	170.8	-0.653
b(T) $\xrightarrow{TS2}$ product 2(T)	0.00	173.48	170.5	-0.653
b(S) $\xrightarrow{TS3}$ product 1(S)	1.71	225.17	168.8	-0.683
b(S) $\xrightarrow{TS4}$ product 2(S)	1.63	173.10	169.8	-0.639
c(T) $\xrightarrow{TS5}$ product 1(T)	3.06	228.65	344.3	-0.986
c(T) $\xrightarrow{TS6}$ product 2(T)	34.27	173.08	183.4	-0.735
c(S) $\xrightarrow{TS7}$ product 1(S)	4.28	225.25	173.0	-0.678
c(S) $\xrightarrow{TS8}$ product 1(S)	35.48	173.06	180.8	-0.734

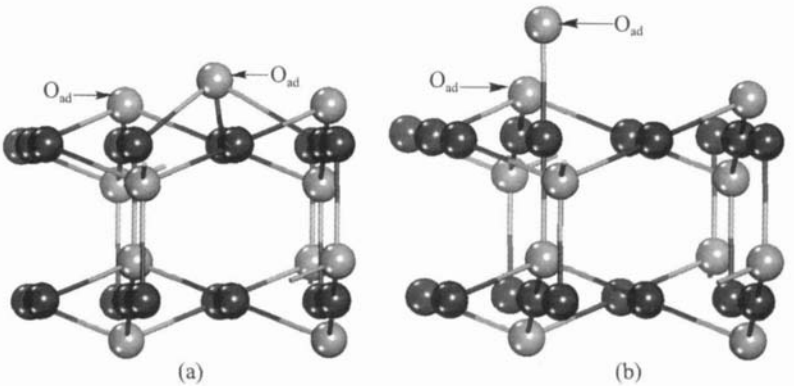

Black circles represent of Cu atoms and the light ones are O atoms

Fig.5 (a) Optimized configuration of product1; (b) Optimized configuration of product2

experimental results[9]. The dissociation reactions for b are easier than those for c. For TS6 and for TS8, they have a small energy barrier, by only 34.27 and 35.48 $kJ \cdot mol^{-1}$, respectively. While the activation energies for other dissociation processes described by TS1 to TS5, and TS7, are all smaller than 2 $kJ \cdot mol^{-1}$, which markedly lower than the barrier for TS6 and TS8. Hence, For TS6 and TS8, they need to surmount a small energy barrier, whereas for other decompositions, they are spontaneous.

The O-O distance and the Mulliken charges of O_2 in TS structures listed in Table 5 also indicate that the O-O bond in TS structures is activated more compared to the reactants, and the O-O bond in products has been completely broken as shown in Fig. 5. Meanwhile, after dissociation of O_2, one of the O_{ad} atoms filled the oxygen defect site, the other lies over Cu_{CUS} site or simultaneo-usly form bonds with three copper atoms (see Fig.5), which is consistent with the above result predicted from atomic oxygen adsorption on Cu_2O (111) surfaces. In contrast, when O_2 dissociates on alkaline-earth oxides, the O_{ad} atoms obtained by dissociation are more favo-rable to adsorb at anion ions, forming peroxide surface species.

3 Conclusions

The adsorption and dissociation of atomic and molecular oxygen at varied adsorption sites on Cu_2O (111) perfect and oxygen deficient surface have been studied employing density functional theory coupled with periodic slab models. The results indicate that for atomic oxygen adsorption, the oxygen defect site is the most preferred site, Cu_{CSA} site is more favorable than Cu_{CUS} site because when O adsorbs at Cu_{CSA} site, the O_{ad} atom is influenced by the nearby cations to form bonds not only with Cu_{CSA} site but also with nearby copper atoms, i.e., Cu_{CUS} and Cu_{CSA}. For molecular oxygen adsorption on perfect (111) surface, O_2 adsorbs preferably end-on to the Cu_{CUS} site and the oxygen species is assigned to the characteristic of the superoxo (O_2^-) type. While for molecular oxygen adsor-ption on deficient (111) surface, they have much larger adsor-ption energy compared to perfect surface and the O-O bonds are stretched significantly, which contributes to the dissociation of O_2, oxygen adspecies is character-istic of a classical O_2^{2-} ion. After optimization, the O-O bond in b has been completely broken, leading to vacancy healing and one O_{ad} adsorbed at Cu_{CUS} site. Such a structure is almost equal to atomic adsorption at Cu_{CUS}. Calculations for O_2 dissociation suggest Cu_2O(111) surface with oxygen deficient exhibits a high cata-lytic reactivity towards O_2 decomposition. The disso-ciative adsorption reaction is highly exothermic. Mean-while the barrier height for dissociation of O_2 over defic-ient (111) surface is calculated to be very small (<2 $kJ \cdot mol^{-1}$), only TS6 and TS8 have relatively larger energy barrier, by 34.27 and 35.48 $kJ \cdot mol^{-1}$, respectively. Furthermore, O_2 dissociates into two O_{ad} atoms, one O_{ad} inserts into the oxygen defect site, the other adsorbs at Cu_{CUS} site or forms bonds with three nearby copper atoms. Our calculation is a worthwhile theoretical example for the interaction of O_2 with Cu_2O.

References:

[1] Henrich V E, Cox P A. The Surface Science of Oxides. Cambridge: Cambridge University Press, 1994.
[2] Witko M. J. Mol. Catal., 1991,70:277~333
[3] Didziulis S V, Butcher K D, Cohen S L. J. Am. Chem. Soc., 1989,111(18):7110~7123
[4] Solomon E I, Jones P M, May J A. Chem. Rev., 1993,93(8):2623~2644
[5] Vissokov G P. Catal. Today, 2004,89(1~2):213~221
[6] Vissokov G P. Catal. Today, 2004,89(1~2):223~231
[7] London J W, Bell A T. J. Catal., 1973,31(1):32~40
[8] Gandhi H S, Shelef M. J. Catal., 1973,28(1):1~7
[9] Schulz K H, Cox D F. Phys. Rev. B, 1991,43:1610~1621
[10]Martinez-Ruiz A, Moreno M, Takeuchi N. Solid State Sci., 2003,5(2):291~295
[11]Jernigan G G, Somorjai G A. J. Catal., 1994,147:567~577
[12]Bordiga S, Paze C, Berlier G, et al. Catal. Today, 2001,70:91~105
[13]Cox D F, Schulz K H. Surf. Sci., 1991,249:138~148
[14]Jones P M, May J A, Solomon E I. Inorg. Chim. Acta, 1998,275~276:327~333
[15]Bredow T, Pacchioni G. Surf. Sci., 1997,373:21~32
[16]Cassarin M, Maccato C, Vittadini A. Chem. Phys. Lett., 1997,280(1~2):53~58
[17]Duan Y H, Zhang K M, Xie X D. Surf. Sci., 1994,321:L249~L254
[18]Soon A, Sohnel T, Idriss H. Surf. Sci., 2005,579(2~3):131~140
[19]Bredow T, Marquez A M, Pacchioni G. Surf. Sci., 1999,430:137~145
[20]Casarin M, Vittadini A. Surf. Sci., 1997,387(1~3):L1079~L1084
[21]Casarin M, Maccato C, Vigato N, et al. Appl. Surf. Sci., 1999,142:164~168
[22]Schulz K H, Cox D F. Surf. Sci., 1992,262:318~334
[23]Rodriguez J A, Hanson J C, Frenkel A I, et al. J. Am. Chem. Soc., 2002,124:346~354
[24]Palmer M S, Neurock M, Olken M M. J. Phys. Chem. B, 2002,106(34):6543~6547
[25]Sensato F R, Custodio R, Calatayud M, et al. Surf. Sci., 2002,511:408~420
[26]Lara-Castells M P D, Krause J L. Chem. Phys. Lett., 2002,354:483~490
[27]Kantorovich L N, Gillan M J. Surf. Sci., 1997,374:373~386
[28]Sueyoshi T, Sasaki T, Iwasawa Y. Surf. Sci., 1996,365:310~318
[29]Xu Y, Mavrikakis M. Surf. Sci., 2001,494:131~144
[30]Perron N, Pineau N, Arquis E, et al. Surf. Sci., 2005,599:160~172
[31]Xu Y J, Li J Q, Zhang Y F, et al. Acta Phys.-Chim. Sin., 2003,19(05):414~418
[32]Wendt S, Schaub R, Matthiesen J, et al. Surf. Sci., 2005,598:226~245
[33]Golovanov V V, Maki-Jaskari M A, Rantala T T. IEEE Seansons Journal, 2002,2:416~421
[34]Matsumoto T, Bennett R A, Stone P, et al. Surf. Sci., 2001,471:225~245
[35]Liem S Y, Kresse G, Clarke J H R. Surf. Sci., 1998,415:194~211
[36]Puisto A, Pitkanen H, Alatalo M, et al. Catal. Today, 2005,100:403~406
[37]Delley B. J. Chem. Phys., 1990,92(1):508~517
[38]Delley B. J. Chem. Phys., 2000,113(18):7756~7764
[39]Perdew J P, Burke K, Ernzerhof M. Phys. Rev. Lett., 1996,77:3865~3868
[40]Perdew J P, Wang Y. Phys. Rev. B, 1992,45:13244~13249
[41]Su M D, Chu S Y. J. Am. Chem. Soc., 1999,121:4229~4237
[42]SUN Bao-Zhen(**孙宝珍**), CHEN Wen-Kai(**陈文凯**), LIU Shu-Hong(**刘书红**), et al. Chinese J. Inorg. Chem.(Wuji Huaxue Xuebao), 2006,22(7):1215~1221
[43]SUN Bao-Zhen(**孙宝珍**), CHEN Wen-Kai(**陈文凯**), XU Xiang-Lan(**徐香兰**). Acta Phys.-Chim. Sin.(Wuli Huaxue Xuebao), 2006,22(9):1126~1131.
[44]Sun B Z, Chen W K, Wang X, et al. Appl. Surf. Sci., 2007,253(18):7501~7505
[45]Chen W K, Liu S H, Cao M J, et al. J. Mol. Struct.(Theochem), 2006,770:87~91
[46]Chen W K, Cao M J, Liu S H, et al. Chem. Phys. Lett., 2006,417:414~418
[47]Chen W K, Lu C H, Chen Z H, et al. Chinese J. Chem. Phys., 2006,19:54~58
[48]Lide D R. Handbook of Chemistry and Physics. 82nd ed., Boca Raton: CRC Press, 2001.
[49]Nakamoto K. Infrared and Raman Spectra of Inorganic and Coordination Compounds. 4th ed., New York: John Wiley and Sons Press, 1986.105
[50]Menetrey M, Markovits A, Minot C, et al. J. Phys. Chem. B, 2004,108:12858~12864